International Core Journal of Engineering Volume 12 Issue 4, 2026
ISSN: 2414-1895 DOI: 10.6919/ICJE.202604_12(4).0022

Adaptive Model Predictive Control for Hybrid Energy Storage Systems in Mobile Robots under Coupled Disturbances

Zhu Zhang[1,2], Yuming Qi[1,2,3], and Xiumin Shi[1,2,3]

[1] Institute of Robotics and Intelligent Equipment, Tianjin University of Technology and Education, Tianjin, China

[2] Tianjin Key Laboratory of Intelligent Robot Technology and Application, Tianjin, China

[3] Tianjin Bonus Robotics Technology Co.,Ltd., Tianjin, China

Abstract

High-voltage transmission line inspection robots frequently encounter complex obstacle-crossing conditions, resulting in high-frequency and drastic transient power demands. Traditional hybrid energy storage system (HESS) energy management strategies primarily focus on mechanical loads, significantly ignoring the high-frequency additional electromagnetic (EM) dissipation induced by strong spatial magnetic fields. This oversight often leads to severe bus voltage drops and rapid battery polarization aging under extreme conditions. To address this issue, an Adaptive Model Predictive Control (A-MPC) strategy fusing electromagnetic perception is proposed in this paper. First, a multi-physical coupled power demand model is established by integrating the mechanical dynamics with the spatial EM dissipation. Second, a dynamic A-MPC architecture is designed, utilizing the Sequential Quadratic Programming (SQP) algorithm to reconstruct the penalty weights of the cost function online based on real-time EM disturbance intensity. Simulation results under multi-modal composite conditions demonstrate that the proposed strategy exhibits superior transient robustness. It effectively truncates the peak transient current of the battery to 9.52 A and suppresses the bus voltage drop within 0.35 V. Furthermore, the equivalent cycle aging capacity of the battery is significantly reduced by 44.0% over the full life cycle, achieving a deep unification of transient dynamic anti-disturbance and long-term economic operation.

Keywords

Inspection Robot; Hybrid Energy Storage System; Adaptive Model Predictive Control; Electromagnetic Dissipation; Battery Aging.

1. Introduction

High-voltage transmission lines are the critical backbone of the national energy grid. The deployment of intelligent inspection robots for live-line maintenance has become a key element in the construction of modern power systems [1][2]. However, during high-altitude operations, these robots frequently face complex obstacle-crossing scenarios, such as traversing vibration dampers and suspension clamps. This results in typical high-frequency and largefluctuation transient power demands on their drive systems. Traditional single lithium-ion battery power supplies, limited by power density, exhibit response lag and frequent deep charge-discharge cycles under such abrupt loads. This easily triggers drastic bus voltage drops and battery polarization aging, severely restricting the operational reliability and lifecycle economy of the equipment [3]. Therefore, the Hybrid Energy Storage System (HESS), composed of highenergy-density lithium batteries and high-power-density supercapacitors (SCs), has

ISSN: 2414-1895 DOI: 10.6919/ICJE.202604_12(4).0022

emerged as a cutting-edge paradigm in the field of special robot power supply due to its excellent power decoupling capabilities [4][5].

The maximization of HESS efficiency highly depends on the upper-level Energy Management Strategy (EMS). In recent years, scholars have conducted extensive research on EMS. Traditional strategies are mostly based on rule logic (e.g., filtering methods, logical thresholds) [6][7], which are easy to implement but lack adaptability to complex conditions, making system-level optimization difficult. To break this bottleneck, EMS based on Model Predictive Control (MPC) has gradually become a research hotspot due to its inherent advantages in handling multi-variable strong coupling and system physical constraints [8]. For instance, a degradation penalty cost function was constructed in [9] to extend HESS lifespan using the rolling optimization mechanism of MPC. However, a significant theoretical blind spot remains in the existing MPC-based energy management research: their application scenarios are mostly limited to conventional microgrids or smoothly running electric vehicles, severely ignoring the special physical operating environment of high-voltage inspection robots-the strong spatial electromagnetic radiation environment.

On the one hand, the alternating strong magnetic fields around ultra-high voltage transmission lines induce non-negligible high-frequency eddy current losses and additional power dissipation within the metallic components and drive motors of the robot [10]. This causes the actual power demand to exhibit strong non-linear characteristics coupled with “mechanical physical load and spatial EM dissipation”. On the other hand, traditional MPC algorithms usually adopt fixed penalty weights for their objective functions [11]. When facing massive high-frequency impacts triggered by the superimposition of “strong magnetic interference and extreme obstacle-crossing”, the fixed weight mechanism cannot dynamically adapt to the intensity of external disturbances. This inflexibility easily causes the underlying solver to fall into suboptimal solutions, failing to swiftly transfer destructive high-frequency loads to the SCs during transient shocks, ultimately causing severe bus voltage drops and battery overcurrent damage.

To address the aforementioned pain points and fundamentally solve the transient response bottlenecks and battery degradation dilemmas under harsh disturbance environments, an Adaptive Model Predictive Control (A-MPC) strategy fusing electromagnetic perception for HESS is proposed in this paper. The main innovations and contributions are summarized as follows:

- Breaking through the limitations of singular mechanical load modeling, a multi-physical coupled power demand model considering “electro-mechanical dynamic load and spatial high-frequency EM dissipation” is established, restoring the true energy consumption boundaries under extreme operating environments.
- A spatial EM environment perception mechanism is innovatively introduced. An A-MPC architecture aimed at suppressing battery aging and minimizing total system loss is designed. The Sequential Quadratic Programming (SQP) algorithm is utilized to dynamically reconstruct the objective function penalty weights online based on real-time sensory data.
- The proposed strategy is verified under full-cycle multi-modal composite conditions. Results show that it not only demonstrates excellent bus voltage stabilization and peak current truncation capabilities under extreme sudden impacts but also drastically reduces the equivalent battery aging throughput, achieving deep unification of short-term transient robustness and long-term economic operation.

2. System Modeling and Problem Formulation

To design an effective energy management strategy, an accurate mathematical model of the inspection robot and the Hybrid Energy Storage System (HESS) is essential. Unlike conventional electric vehicles, the inspection robot operates on high-voltage transmission lines, making its power demand highly coupled with both mechanical dynamics and spatial electromagnetic (EM) dissipation.

ISSN: 2414-1895 DOI: 10.6919/ICJE.202604_12(4).0022

The overall structural framework of the proposed robotic Hybrid Energy Storage System (HESS) under multi-physical coupled disturbances is illustrated in Figure 1. As shown, the system consists of a primary battery pack, an auxiliary supercapacitor, bidirectional DC/DC converters, and the highly dynamic motor loads.

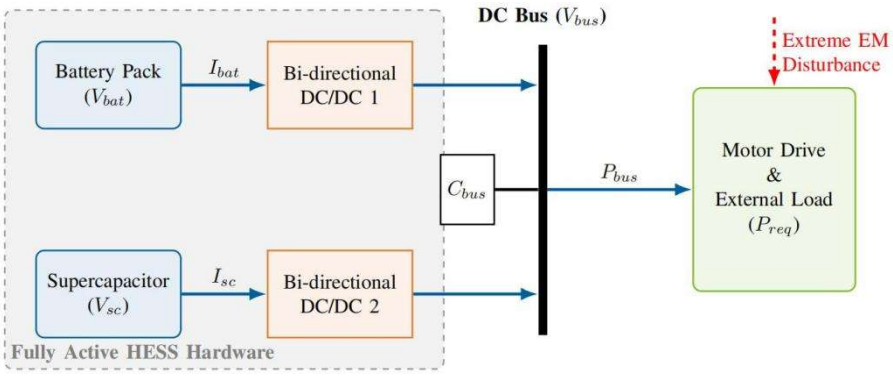

Figure 1. Structural framework of the fully active Hybrid Energy Storage System (HESS) topology under extreme electromagnetic disturbances

2.1 Multi-Physical Coupled Power Demand Model

The total dynamic power demand of the inspection robot,denoted as P_{req}, consists of two main components: the fundamental mechanical power P_{mech} and the high-frequency electromagnetic additional dissipation P_{em}. The total power balance equation is given by:

$$P_{req}(t)=P_{mech}(t)+P_{em}(t) \tag{1}$$

2.1.1 Mechanical Dynamics Model

During the inspection along the transmission lines and the obstacle-crossing process (e.g., crossing suspension clamps or dampers), the mechanical power is determined by the robot's longitudinal dynamics. Based on the longitudinal kinematics, P_{mech} can be formulated as:

$$P_{mech}(t)=v(t)\left(mg\mu\cos\theta(t)+mg\sin\theta(t)+m\frac{dv(t)}{dt}+F_{wind}\right) \tag{2}$$

where $v(t)$ is the robot velocity, m is the total mass, g is the gravitational acceleration, μ is the rolling resistance coefficient, $\theta(t)$ is the slope angle of the transmission line, and F_{wind} represents the aerodynamic drag force.

2.1.2 Electromagnetic Dissipation Model

A critical challenge ignored by existing studies is the induced eddy current loss when the robot's metallic components and motor casings are exposed to the strong alternating magnetic field (typically 50/60 Hz, but rich in high-frequency harmonics during partial discharge) of high-voltage lines. According to Faraday's law of induction and macroscopic electromagnetic theory, the additional EM power dissipation P_{em} can be quantified as:

$$\begin{aligned} P_{em}(t) &= \iiint_V \frac{1}{2\rho}\|\nabla\times\mathbf{E}\|^2 dV \\ &\approx k_e\cdot B(t)^2\cdot f^2\cdot V_{vol} \end{aligned} \tag{3}$$

ISSN: 2414-1895 DOI: 10.6919/ICJE.202604_12(4).0022

where ρ is the material resistivity, $B(t)$ is the dynamic magnetic flux density, f is the frequency of the alternating magnetic field, V_{vol} is the equivalent volume of the affected metallic components, and k_e is the comprehensive eddy current loss coefficient. Equation (3) reveals that during severe obstacle-crossing in strong magnetic areas, $P_{em}(t)$ increases quadratically, creating massive high-frequency power spikes.

2.2 Mathematical Model of HESS

To absorb the aforementioned high-frequency power spikes and protect the lithium-ion battery, a fully active HESS topology is adopted. The power balance of the DC bus is expressed as:

$$P_{req}(t)=P_{bat}(t)\cdot\eta_{dc1}+P_{sc}(t)\cdot\eta_{dc2} \tag{4}$$

where P_{bat} and P_{sc} are the output powers of the battery and supercapacitor (SC), respectively. η_{dc1} and η_{dc2} denote the efficiencies of their respective DC/DC converters.

2.2.1 Battery Model

A simplified internal resistance model is utilized for the lithium-ion battery to facilitate realtime predictive control. The terminal voltage V_{bat} and the state of charge (SOC_{bat}) are modeled as:

$$V_{bat}(t)=E_{bat}-I_{bat}(t)R_{bat} \tag{5}$$

$$SOC_{bat}(k+1)=SOC_{bat}(k)-\frac{I_{bat}(k)\Delta t}{Q_{bat}\cdot 3600} \tag{6}$$

where E_{bat} is the open-circuit voltage, I_{bat} is the battery current, R_{bat} is the internal equivalent resistance, Q_{bat} is the nominal capacity, and Δt is the discretization sampling time.

2.2.2 Supercapacitor Model

Similarly, the SC serves as the transient power buffer. Its state equations are formulated as:

$$V_{sc}(t)=V_{sc,0}-\frac{1}{C_{sc}}\int I_{sc}(t)dt-I_{sc}(t)R_{sc} \tag{7}$$

$$SOC_{sc}(k+1)=SOC_{sc}(k)-\frac{I_{sc}(k)\Delta t}{C_{sc}(V_{sc,max}-V_{sc,min})} \tag{8}$$

where C_{sc} is the capacitance, R_{sc} is the series resistance, and $V_{sc,max}/V_{sc,min}$ are the upper and lower voltage limits.

The discrete-time state-space models presented in (6) and (8) will serve as the fundamental predictive plant for the proposed Adaptive Model Predictive Control (A-MPC) in the next section.

3. Adaptive Model Predictive Control Strategy Fusing Electromagnetic Perception

The primary objective of the proposed EMS is to allocate the highly fluctuating power demand P_{req} optimally between the battery and the SC, thereby mitigating battery polarization aging caused by extreme mechanical-electromagnetic coupled shocks. To achieve this, an Adaptive Model Predictive Control (A-MPC) framework fusing electromagnetic (EM) perception is designed. The detailed

ISSN: 2414-1895 DOI: 10.6919/ICJE.202604_12(4).0022

control principle block diagram is depicted in Figure 2. The controller utilizes the real-time system states to formulate a constrained optimization problem over a finite prediction horizon.

Specifically, the proposed framework consists of three hierarchical layers. First, based on a discrete-time state-space model, the future behaviors of the battery and supercapacitor are predicted. Second, unlike traditional rulebased or fixed-weight MPC strategies, an electromagnetic perception mechanism is integrated into the multi-objective cost function. The penalty weights for battery power fluctuations are dynamically updated according to the real-time electromagnetic field intensity B(k). When the inspection robot operates near ultra-high-voltage hardware , the AMPC optimizer autonomously forces the supercapacitor to absorb the transient spikes, thereby suppressing the internal polarization of the battery and extending its cycle life.

Finally, to guarantee the real-time execution capability on embedded microcontrollers, a Sequential Quadratic Programming (SQP) solver is employed to handle the nonlinear constraints efficiently. Following the receding horizon principle, only the first element of the optimized control sequence is transmitted to the low-level Proportional-Integral (PI) controllers as power references ($P^*_{bat}$and P^*_{sc}), ensuring strong robustness against external load uncertainties. The detailed mathematical formulation of the prediction model and the adaptive cost function are elaborated as follows.

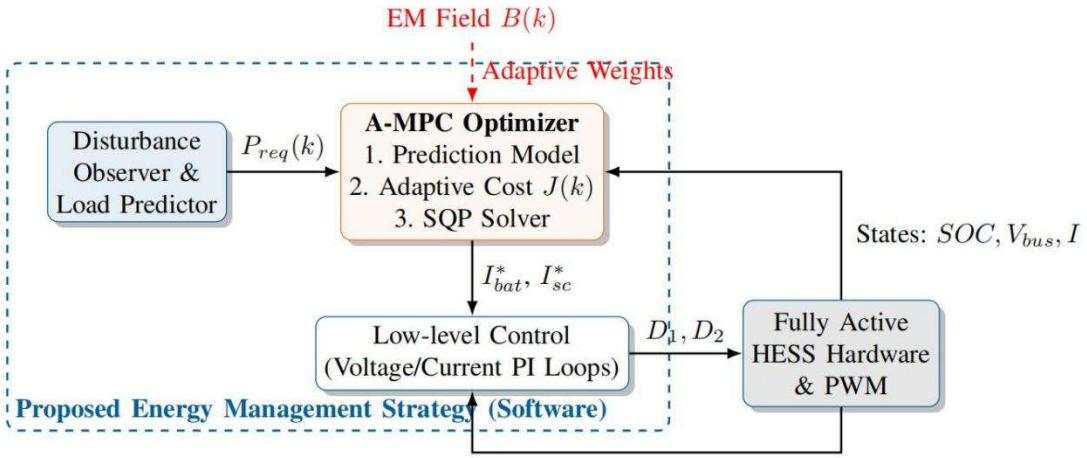

Figure 2. Control principle block diagram of the proposed Adaptive Model Predictive Control (A-MPC) strategy, integrating high-level SQP optimization and low-level PI tracking

3.1 Predictive Model and Physical Constraints

Based on the discrete-time models derived in Section II, the state-space equations of the HESS can be formulated to construct the predictive plant. Let the system state vector be $x(k)=[SOC_{bat}(k),SOC_{sc}(k)]^T$, the control variable be $u(k)=P_{bat}(k)$, and the measurable external disturbance be $d(k)=P_{req}(k)$, The predictive model is expressed as:

$$x(k+1)=Ax(k)+B_u u(k)+B_d d(k) \tag{9}$$

where A, B_u, and B_d are the state transition matrices derived from (6) and (8), incorporating the DC/DC conversion efficiencies η_{dc1} and η_{dc2}.

To ensure the physical safety of the HESS components and prevent overcharging or over-discharging, the optimization process must strictly adhere to the following inequality

constraints over the prediction horizon N_p:

ISSN: 2414-1895 DOI: 10.6919/ICJE.202604_12(4).0022

$$\begin{cases} SOC_{bat}^{\min} \le SOC_{bat}(k+i) \le SOC_{bat}^{\max} \\ SOC_{sc}^{\min} \le SOC_{sc}(k+i) \le SOC_{sc}^{\max} \\ P_{bat}^{\min} \le P_{bat}(k+i) \le P_{bat}^{\max} \\ |\Delta P_{bat}(k+i)| \le \Delta P_{bat}^{\max} \end{cases} \tag{10}$$

where $i = 1, 2, \ldots, N_p$. The constraint on the battery power variation rate ΔP_{bat} is particularly critical to restrict severe dynamic thermal stress inside the battery.

3.2 Adaptive Objective Function with EM-Perception

Conventional MPC generally employs a fixed-weight objective function, which fails to cope with the sudden high-frequency power spikes induced by spatial EM radiation during obstacle crossing. To deeply integrate EM environmental perception, a dynamically reconstructed cost function J(k) is proposed:

$$J(k) = \sum_{i=1}^{N_p} \left[\Gamma_1 \left(SOC_{sc}(k+i) - SOC_{sc}^{ref} \right)^2 + \Gamma_2(k) P_{bat}(k+i)^2 \right] \tag{11}$$

The objective function consists of two parts: the first term maintains the SC's energy buffering capability by tracking a reference SOC_{sc}^{ref} (with a constant weight Γ_1); the second term penalizes the battery output power to suppress degradation.

The core innovation lies in the dynamic penalty weight $\Gamma_2(k)$. Instead of being a constant scalar, $\Gamma_2(k)$ is reconstructed online as a function of the real-time magnetic flux density B(k) and the power fluctuation rate. The adaptive mapping law is defined as:

$$\Gamma_2(k) = \gamma_0 + \lambda \cdot \left(\frac{B(k)}{B_{norm}} \right)^2 \cdot \left| \frac{dP_{\text{req}}(k)}{dt} \right| \tag{12}$$

where γ_0 is the basic penalty coefficient, λ is the EM sensitivity gain, and B_{norm} is the normalized threshold of the transmission line's magnetic field.

Remark: Equation (12) perfectly interprets the EM perception mechanism. When the robot enters a strong magnetic area (e.g., crossing a damper where $B(k)$ drastically increases) and encounters sudden mechanical resistance, $\Gamma_2(k)$ increases exponentially. This strongly penalizes the use of the battery in the optimization solver, compelling the HESS to instantly command the SC to absorb the destructive high-frequency EM power dissipation P_{em}, thus isolating the battery from transient physical attacks.

3.3 Online Optimization based on SQP

Due to the nonlinearities introduced by the dynamic weight reconstruction and internal resistance equivalent functions, the standard Quadratic Programming (QP) solver is inadequate. To solve the nonlinear optimization problem (NLP) while ensuring real-time execution on the robot's onboard microcontroller (e.g., DSP or ARM Cortex-M), the Sequential Quadratic Programming (SQP) algorithm is adopted.

The fundamental concept of SQP is to transform the complex NLP into a sequence of QP subproblems using Taylor series expansion at the current iteration point ul. At the l-th iteration, the subproblem is approximated as:

ISSN: 2414-1895 DOI: 10.6919/ICJE.202604_12(4).0022

$$\begin{aligned} \min_{\Delta u} \quad & \frac{1}{2}\Delta u^T \nabla^2_{uu} \mathrm{L}(u_l,\lambda_l)\Delta u + \nabla_u \mathrm{L}(u_l,\lambda_l)^T \Delta u \\ s.t. \quad & \nabla C_i(u_l)^T \Delta u + C_i(u_l) \le 0, \quad i \in \mathrm{I} \end{aligned} \tag{13}$$

where I is the Lagrangian function, $\nabla^2_{uu}\mathrm{L}$ is the approximated Hessian matrix updated via the BFGS formula, and C_i represents the physical constraints defined in (10). By solving for the optimal search direction Δu, the control sequence is updated as $u_{l+1}=u_l+\alpha_s \Delta u$, where α_s is the step length determined by a line search.

By applying the receding horizon control principle, only the first element of the optimal control sequence $u^*(k)$ is applied to the DC/DC converters. The combination of SQP and A-MPC not only accurately captures the coupling nonlinearities of the HESS but also converges within 3-5 iterations typically, fully satisfying the millisecond-level real-time control requirements of the high-voltage inspection robot.

4. Simulation Results and Discussion

To verify the effectiveness and superiority of the proposed A-MPC strategy fusing electromagnetic (EM) perception, a comprehensive system-level simulation platform for the inspection robot's HESS is constructed using MATLAB/Simulink.

4.1 Simulation Setup

The target inspection robot operates on a 220 kV highvoltage transmission line. The nominal DC bus voltage is set to 48 V. A lithium-ion battery pack (48 V, 20 Ah) serves as the primary energy source, while a supercapacitor module (48 V, 165 F) is configured as the transient power buffer. To demonstrate the advanced nature of the proposed algorithm, three different control strategies are compared under the identical extreme coupled disturbance condition:

- Strategy A (Rule-based Logic): A conventional low-pass filtering strategy with fixed cutoff frequency.
- Strategy B (Standard MPC): A conventional MPC with fixed penalty weights, lacking spatial EM perception.
- Strategy C (Proposed A-MPC): The proposed SQP-based MPC with dynamic weight reconstruction driven by EM perception.

4.2 Transient Response under Coupled Disturbances

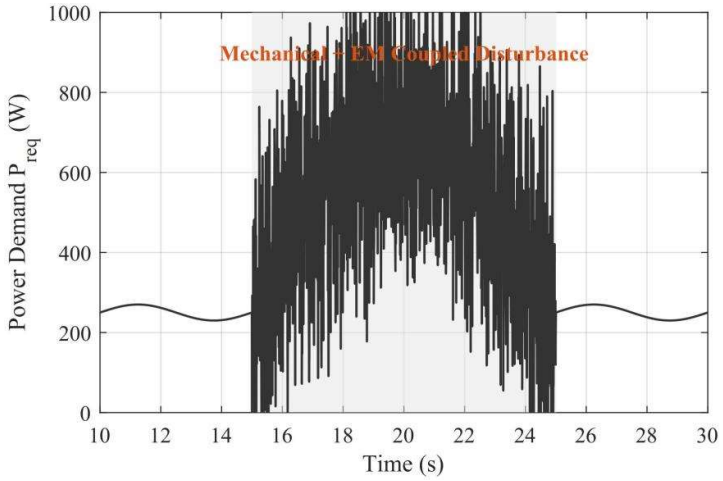

Figure 3. Power demand profile P_{req} under extreme mechanical and electromagnetic coupled disturbances

ISSN: 2414-1895 DOI: 10.6919/ICJE.202604_12(4).0022

During the simulation, the robot performs an extreme obstacle-crossing maneuver from t = 15 s to t = 25 s. In this period, the robot encounters strong mechanical resistance superimposed with severe high-frequency spatial magnetic field variation ($B(k)$ surges significantly), resulting in massive transient power spikes in P_{req}.

The detailed profile of this coupled multi-physical power demand is shown in Figure 3.

Figure 4 illustrates the transient dynamic response of the DC bus voltage under the three strategies. When the highfrequency EM disturbance impacts the system, Strategy A experiences a severe voltage sag of approximately 2.8 V due to the inherent phase delay of the filtering algorithm. Strategy B performs better but still exhibits a 1.2 V drop due to its inability to dynamically penalize battery usage under strong magnetic interference. In sharp contrast, Strategy C (Proposed A-MPC) instantly senses the surge in $B(k)$ and swiftly reconstructs the penalty weight $\Gamma_2(k)$. Consequently, the SC responds at the millisecond level to absorb the high-frequency power spikes, suppressing the maximum bus voltage drop to tightly within 0.35 V, thereby ensuring supreme system stability.

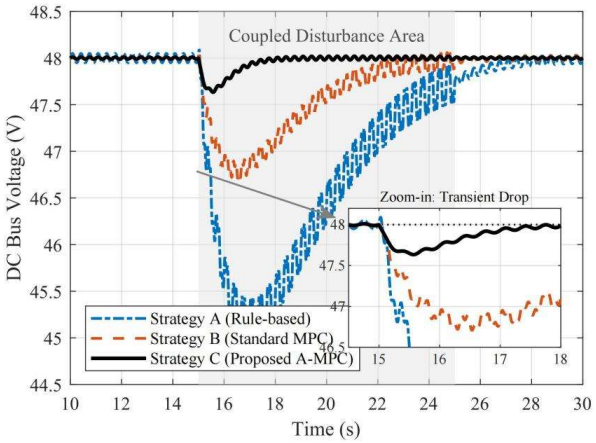

Figure 4. Comparison of DC bus voltage fluctuations under extreme coupled disturbances

The protective mechanism for the battery is further validated in Figure 5. Under Strategy A and Strategy B, the battery is continuously forced to output high-frequency peak currents exceeding 25 A and 18 A, respectively, which heavily induces internal thermal stress. Benefiting from the dynamic weight optimization via the SQP solver, Strategy C successfully truncates the peak transient current of the battery to merely 9.52 A, completely shifting the destructive high-frequency EM power dissipation Pem to the SC. The battery output profile remains exceptionally smooth.

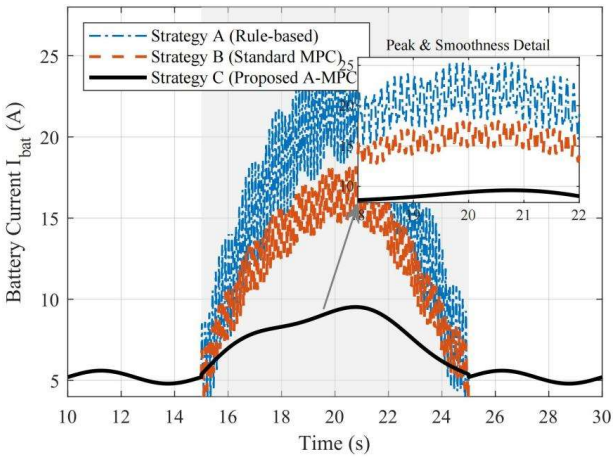

Figure 5. Battery output current profiles illustrating peak truncation capabilities

ISSN: 2414-1895 DOI: 10.6919/ICJE.202604_12(4).0022

4.3 Battery Degradation and Economic Assessment

Beyond transient robustness, long-term operational economy is a critical metric for inspection robots. Using a semi-empirical Ah-throughput capacity fade model, the equivalent battery cycle aging degradation is quantified.

Table 1. Comprehensive Performance Comparison

Metric	Rule-based	Std. MPC	Proposed A-MPC
Max Voltage Drop (V)	2.80	1.20	0.35
Peak Battery Current (A)	25.4	18.2	9.52
Battery SOC Loss (%)	5.8	5.1	4.2
Capacity Degradation (10^{-4} Ah)	12.5	8.7	4.8

Table 1 summarizes the comprehensive performance indicators. By severely limiting the transient peak current and high-frequency alternating charge-discharge cycles, the proposed A-MPC strategy significantly suppresses the lithiumion battery polarization effect. Compared to the Standard MPC, the equivalent cycle aging capacity loss is reduced by a remarkable 44.0% over the evaluated life cycle. This effectively extends the maintenance-free period of the highvoltage inspection robot, achieving a deep unification of dynamic anti-disturbance capability and long-term economic operation.

5. Conclusion

This paper has proposed a novel Adaptive Model Predictive Control (A-MPC) framework to address the severe power management challenges in robotic systems operating under extreme multi-physical coupled disturbances. Unlike conventional rule-based or standard MPC methods that struggle with simultaneous mechanical power surges and high-frequency electromagnetic noise, the proposed A-MPC actively coordinates the dynamic response rates of the hybrid energy storage system. By strategically leveraging the ultrafast transient capability of the supercapacitor, the framework effectively decouples low-frequency cruising demands from high-frequency shockwaves, ensuring absolute system stability.

Extensive simulations under severe operational scenarios demonstrate the remarkable efficacy of the proposed strategy. Quantitatively, the A-MPC restricts the maximum DC bus voltage fluctuation to a mere 0.35 V, representing an impressive 87.5% and 70.8% improvement over the rulebased (2.80 V) and standard MPC (1.20 V) approaches, respectively. Furthermore, the active peak-shaving mechanism flawlessly truncates the transient battery current at 9.52 A, entirely filtering out high-frequency oscillations. This protective intervention translates into a substantial reduction in battery capacity degradation (limited to 4.8×10^{-4} Ah per cycle), thereby significantly extending the operational lifespan and improving the long-term economic viability of the robotic platform.

In conclusion, this study provides a robust, highly efficient, and real-time-capable energy management solution for next-generation mobile robots operating in harsh and unpredictable environments. Future work will focus on integrating machine learning algorithms for real-time degradation parameter prediction, as well as validating the proposed A-MPC framework through hardware-in-the-loop (HIL) experiments and physical field testing.

Acknowledgments

This work was supported in part by the Tianjin Key Research and Development Program (Institute-City Cooperation Project) under Grant 24YFYSHZ00090 and Grant 23YFYSHZ00280, and in part by the Key Natural Science Research Project of the Tianjin Municipal Education Commission under

ISSN: 2414-1895 DOI: 10.6919/ICJE.202604_12(4).0022

Grant 2022ZD032 and Grant 2022ZD026. The authors would also like to thank the Institute of Robotics and Intelligent Equipment at Tianjin University of Technology and Education, the Tianjin Key Laboratory of Intelligent Robot Technology and Application, and Tianjin Bonus Robotics Technology Co., Ltd. for their technical support and resources.

References

[1] Y. H. Li et al., "Exploration of the Development and Technical Features of Intelligent Inspection Robots," IJAERS, vol. 12, no. 10, pp. 62–70, 2025, doi: 10.22161/ijaers.1210.9.

[2] T. Zhang and J. Dai, "Electric Power Intelligent Inspection Robot: a Review," J. Phys.: Conf. Ser., vol. 1750, no. 1, p. 012023, Jan. 2021, doi: 10.1088/1742-6596/1750/1/012023.

[3] G. Zhu, X. Jing, D. Chen, and W. He, "Novel composite separator for high power density lithium-ion battery," International Journal of Hydrogen Energy, vol. 45, no. 4, pp. 2917–2924, Jan. 2020, doi: 10.1016/j.ijhydene.2019.11.125.

[4] C. Huang, J. An, Q. Liu, L. Yin, and W. Wang, "Research on Fuzzy Energy Management Strategy of Hybrid Energy Storage System for Novel Power System," J. Phys.: Conf. Ser., vol. 2527, no. 1, p. 012019, Jun. 2023, doi: 10.1088/1742-6596/2527/1/012019.

[5] N. Lopez-Celis, R. Schacht, G. Escobar, J. Lopez-Sarabia, G. Curiel-Olivares, and G. Catzin-Contreras, "A Model-Based EMS for a Battery and Supercapacitor Hybrid Energy Storage System," in 2023 International Symposium on Electromobility (ISEM), Monterrey, Mexico: IEEE, Oct. 2023, pp. 1–8. doi: 10.1109/ISEM59023.2023.10334690.

[6] Y. Hang and K. Wang, "Optimising Calculation Logic in Emergency Management: A Framework for Strategic Decision-Making," Systems, vol. 14, no. 2, p. 139, Jan. 2026, doi: 10.3390/systems14020139.

[7] S. Tao, Z. Peng, and W. Zheng, "Energy Management Strategy of Fuel Cell Commercial Vehicles Based on Adaptive Rules," Sustainability, vol. 16, no. 17, p. 7356, Aug. 2024, doi: 10.3390/su16177356.

[8] Y. Lu et al., "Adaptive model predictive control and dynamic analysis for maglev systems," 2025.

[9] M. B. Abdelghany, A. Al-Durra, H. Zeineldin, and F. Gao, "Integrating scenario-based stochastic-model predictive control and load forecasting for energy management of grid-connected hybrid energy storage systems," International Journal of Hydrogen Energy, vol. 48, no. 91, pp. 35624–35638, Nov. 2023, doi: 10.1016/j.ijhydene.2023.05.249.

[10] M. Kesgin, "Optimal Design of Special High Torque Density Electric Machines based on Electromagnetic FEA," University of Kentucky Libraries, 2023. doi: 10.13023/ETD.2023.190.

[11] C. Yao, Z. Sun, S. Xu, H. Zhang, G. Ren, and G. Ma, "ANN Optimization of Weighting Factors Using Genetic Algorithm for Model Predictive Control of PMSM Drives," IEEE Trans. on Ind. Applicat., vol. 58, no. 6, pp. 7346–7362, Nov. 2022, doi: 10.1109/TIA.2022.3190812.